Magneto-optical effects from nanophase α-Fe and Fe_3O_4 precipitates formed in yttrium-stabilized ZrO_2 by ion implantation and annealing

S. Honda, F. A. Modine, A. Meldrum, J. D. Budai, T. E. Haynes, and L. A. Boatner[a)]
Solid State Division, Oak Ridge National Laboratory, Oak Ridge, Tennessee 37831

(Received 22 February 2000; accepted for publication 6 June 2000)

Magneto-optically active nanocomposite structures have been created by using ion implantation and thermal processing to form precipitated layers of ferromagnetic α-Fe or ferrimagnetic Fe_3O_4 that are embedded in the near-surface region of (100)-oriented yttrium stabilized ZrO_2 (YSZ). When Fe-implanted YSZ is annealed at 1100 °C in Ar+4%H_2, the redox conditions are sufficiently reducing so that metallic Fe is the stable phase. At lower temperatures the annealing conditions become less reducing and Fe_3O_4 becomes the stable phase. Transmission electron microscopy and x-ray diffraction studies established that each α-Fe or Fe_3O_4 particle is a single crystal that is crystallographically aligned with respect to the YSZ host. Magneto-optical effects due to both the α-Fe and Fe_3O_4 nanophase precipitates were found and characterized using magnetic circular dichroism. These magneto-optical effects have potential applications in integrated-optical devices.
© *2000 American Institute of Physics.* [S0003-6951(00)02031-3]

Recent work has shown that ion implantation and thermal processing techniques can be used to form embedded nanophase precipitates whose properties change significantly either at a phase transition or when subjected to an external perturbation.[1–3] These property changes can result in the formation of either ''smart'' or ''active'' nanocomposites in the near-surface region of host materials that would otherwise be inactive.[3] (Here, a smart surface combines both sensing and actuating functions while an active surface has properties that respond to a deliberately applied external perturbation.) In the present work, the concept of creating active or smart near-surface nanocomposites on inactive materials is extended to encompass the formation of surfaces containing dispersed but crystallographically oriented and faceted single-crystal magnetic nanophase precipitates. These magnetic nanocomposite surfaces were found to exhibit an unusual type of magneto-optical activity arising from the interaction of light with the dispersed precipitates resulting in the creation of an optically active layer on the surface of the otherwise inactive cubic zirconia host.

Ion implantation and annealing were used to form nanophase magnetic precipitates of either metallic α-Fe or Fe_3O_4 (magnetite) that are embedded in the surface of an yttrium-stabilized, cubic ZrO_2 (YSZ) host. The Fe^+ ions were implanted into a Syton-polished, (100)-oriented surface of $Y_{0.15}Zr_{0.85}O_{1.93}$ using an implant energy of 140 keV, a dose of 8.0×10^{16} Fe^+ ions/cm^2, and a sample temperature of ~77 K. Calculations carried out using the TRIM code[4] predict that the peak of the Fe-implant profile is at a depth of ~45 nm below the surface. Following the implantation of Fe^+, thermal treatments in a reducing atmosphere were carried out to induce the precipitate formation. When the Fe-implanted YSZ crystals were annealed at 1000 °C for 1 h in Ar+4%H_2 and then slowly cooled to room temperature the redox conditions at the lower temperatures were such that Fe_3O_4 was the stable phase and ~3–9 nm magnetite particles were formed that were crystallographically oriented with respect to the YSZ lattice. When the samples containing the Fe_3O_4 precipitates were heated for 2 h in Ar+4%H_2 at 1100 °C, the conditions were sufficiently reducing so that metallic Fe was the stable phase which could be retained by quenching the samples from 1100 °C. This resulted in the formation of cubic faceted, ~10–20 nm single-crystal precipitates of metallic Fe that were crystallographically oriented with respect to the host YSZ lattice—and accordingly with each other.

The plan-view transmission electron microscope (TEM) images shown in Fig. 1(a) illustrate the generally cubic morphology and size distribution characteristic of the faceted, aligned α-Fe precipitates formed in YSZ. The TEM micrograph in Fig. 1(b) shows a high-resolution image of a single large and several smaller iron particles, and the Moiré fringe contrast establishes that the single-crystal precipitates are aligned with the host YSZ lattice. X-ray diffraction analysis of the Fe-precipitate/YSZ-host system confirmed the formation of metallic α-Fe and also revealed the presence of a small component of γ-Fe even though the Fe phase diagram shows that the γ-Fe phase is not normally stable at room temperature. X-ray analysis was also used to determine that the α-Fe precipitates exhibit two different, but symmetry related, orientations relative to the YSZ host. The predominant orientation is: α-Fe(110)‖YSZ(001) out-of-plane and α-Fe[001]‖YSZ[100] in-plane. The less-common relative orientation was found to be: α-Fe(001)‖YSZ(001) out-of-plane and α-Fe[100]‖YSZ[110] in-plane. The particles of the small γ-Fe component had only one relative orientation that was determined to be: γ-Fe(001)‖YSZ (001) out-of-plane and γ-Fe[100]‖YSZ[100] in-plane.

A plan-view TEM micrograph of the Fe_3O_4 precipitates is shown in Fig. 2(a). A comparison of Figs. 1(a) and 2(a) illustrates the significant difference between the sizes of the metallic α-Fe precipitates and the magnetite particles. Electron diffraction analysis established that the Fe_3O_4

[a)]Electronic mail: lb4@ornl.gov

 © 2000 American Institute of Physics
Downloaded 11 Sep 2009 to 160.91.157.167. Redistribution subject to AIP license or copyright; see http://apl.aip.org/apl/copyright.jsp

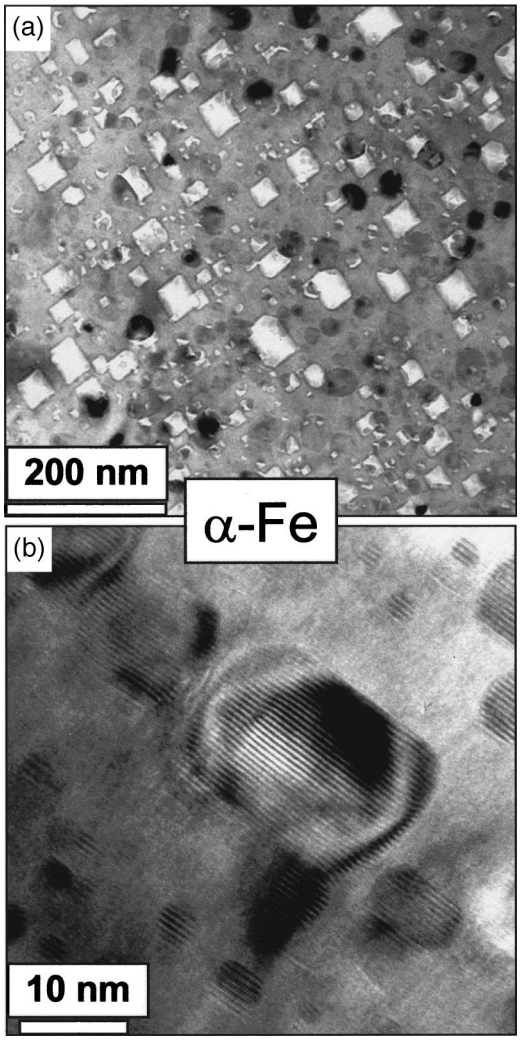

FIG. 1. (a) TEM micrograph of a backthinned sample of YSZ containing faceted, coherently oriented predominantly α-Fe nanophase particles [viewing direction along the YSZ (100) axis]. (b) High-magnification view showing Moiré fringes consistent with the crystallographic orientation of the precipitates relative to the host YSZ lattice.

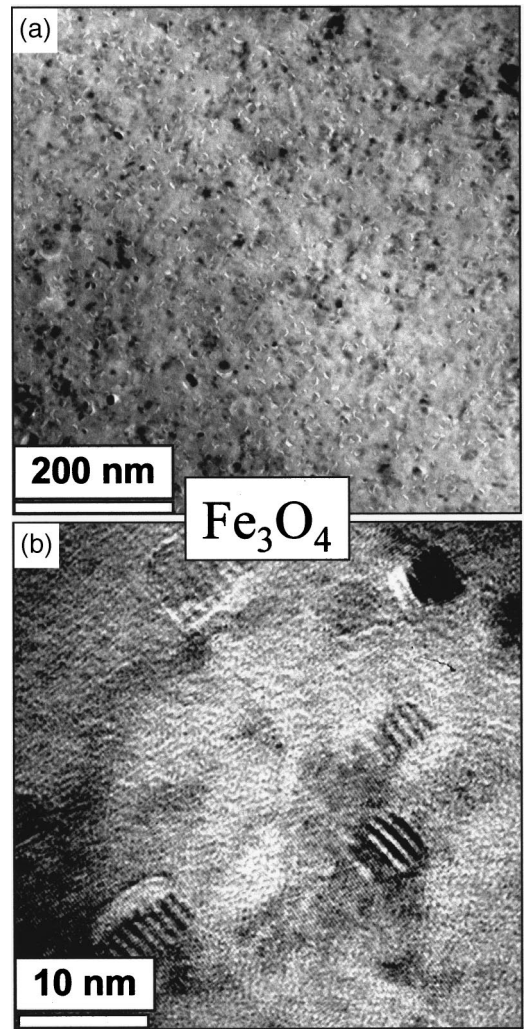

FIG. 2. (a) TEM micrograph of a backthinned sample of YSZ containing nanophase precipitates of Fe_3O_4. (b) High-magnification view showing the details of the Fe_3O_4 particle morphology. The Moiré fringes show that the Fe_3O_4 precipitates are crystallographically aligned relative to the YSZ host crystal lattice.

particles were oriented cube-on-cube with respect to the YSZ host lattice. The presence of Moiré fringes in the higher-magnification TEM micrograph shown in Fig. 2(b) also indicates that the Fe_3O_4 particles are crystallographically oriented with respect to the YSZ host-crystal lattice. X-ray analysis confirmed the presence of Fe_3O_4 particles and showed that the relative particle-host orientation was, in fact: $Fe_3O_4(001)\|YSZ(001)$ out-of-plane and $Fe_3O_4[100]\|YSZ[100]$ in-plane.

By introducing embedded nanophase precipitates of α-Fe or Fe_3O_4, it was possible to create a magneto-optically active layer in the otherwise optically inactive near-surface region of the YSZ host crystal. These magnetic-precipitate-induced magneto-optical effects were manifested in the form of the relatively large magnetic circular dichroism (MCD) response illustrated in Fig. 3. MCD signals like those in Fig. 3 represent the magnetically induced difference in the absorption of right- and left-circularly polarized light by the magnetic nanocomposite surface. Since the boundaries of the region occupied by the magnetic particles are diffuse, the MCD signal is defined in terms of the optical density of the precipitate/host system as follows:

$$\mathrm{MCD}=\mathrm{OD}_L-\mathrm{OD}_R=\log_{10}(e)\int_0^{\infty}(\alpha_L-\alpha_L)dt, \qquad (1)$$

where α_L and α_R are the absorption coefficient for left- and right-circularly polarized light, t is the thickness of the implanted layer, and OD_L and OD_R are the optical density for left- and right-circularly polarized light, respectively.

The magnetic-field variations of the MCD measured at a wavelength of 400 nm for the α-Fe and Fe_3O_4/YSZ near-surface nanocomposite systems are shown in Fig. 3 for sample temperatures of 297 and 4 K. An analysis of the MCD response for magnetic nanoparticles will be presented elsewhere.[5] The MCD has been shown to be proportional to the magnetization of the particles,[5] so the hysteresis loops in Fig. 3 can be explained in terms of the magnetic characteristics of small embedded particles. The coercivities and remanents (i.e., MCD response that remains when a high magnetic field is returned to zero) are shown on the figure. Variations in the coercivity of both the α-Fe and Fe_3O_4 particles as a function of temperature are apparent in Fig. 3.

The sample coercivities can be attributed to the cubic magnetocrystalline anisotropy of single crystals in crystallo-

Downloaded 11 Sep 2009 to 160.91.157.167. Redistribution subject to AIP license or copyright; see http://apl.aip.org/apl/copyright.jsp

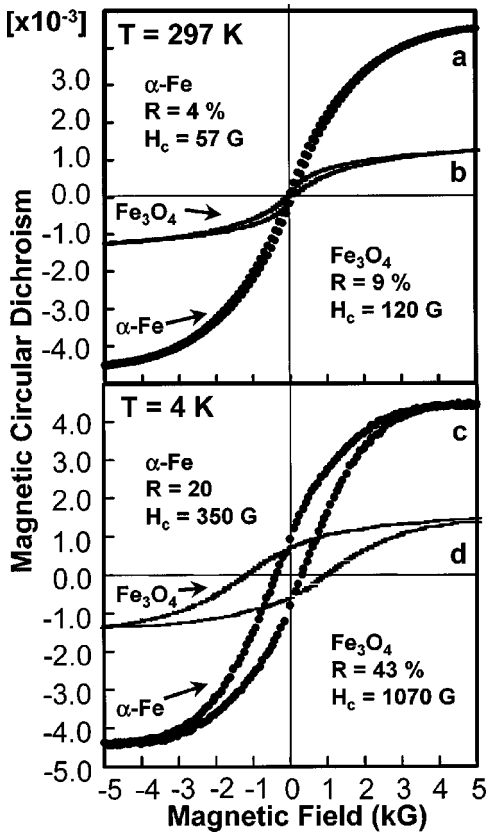

FIG. 3. MCD results showing the hysteretic response of magnetic α-Fe and Fe_3O_4 precipitates in a single crystal YSZ host. Curves *a* and *c* show the MCD results for Fe at 297 and 4 K, respectively, while curves *b* and *d* show the results for Fe_3O_4 at these temperatures. The coercivity, H_c, and a factor, R, representing the ratio of the remanent response at $H=0$ to the saturation value at high H, are indicated.

graphic alignment with the YSZ host. The α-Fe particles have two alignments relative to the applied magnetic field, i.e., ~2/3 of the α-Fe particles have a [110] axis along the field direction and about 1/3 have a [100] axis along the field direction. The coercivities at $T=0$ for particles with these alignments are

$$H_{CO[100]}=2K/M_s, \tag{2a}$$

$$H_{CO[110]}=(2/3)^{3/2}K/M_s, \tag{2b}$$

where K is the anisotropy constant, and M_s is the saturation magnetization.

The Fe_3O_4 particles are in a cube-on-cube alignment with the YSZ so their coercivity is

$$H_{CO}=H_{CO[100]}=(2/3)^{3/2}K/M_s. \tag{3}$$

[The particle directions in Eqs. (2b) and (3) are different because K is negative for Fe_3O_4 but positive for α-Fe.] The small particles are expected to become superparamagnetic above a blocking temperature T_b that depends upon their volume V

$$T_b \cong KV/100k_B. \tag{4}$$

Table I shows estimates of H_{CO} and T_b obtained from Eqs. (2) to (4) by using the average particle volumes $\overline{V}$ (from TEM) and K values obtained from Mössbauer measurements.[6,7] The bulk K values are included.

TABLE I. Estimates of H_{CO} and T_b for α-Fe and Fe_3O_4 particles in YSZ.

Particle	M_s (G)	K_{bulk} (10^5 erg/cm^3)	$K_{Möss}$ (10^5 erg/cm^3)	$\overline{V}$ (10^{-18} cm^3)	H_{CO} (G)	T_b (K)
α-Fe	1710	4.8	8.2	6.0	493	356
Fe_3O_4	510	−11.0	−12.0	0.5	1280	43

The coercivities of α-Fe and Fe_3O_4 measured at 4 K, where all of the particles should be blocked, are in reasonable agreement with the H_{CO} estimates, since a 4 K value is expected to be at least 10% less than H_{CO} because of thermal effects. The value of $T_b=356$ K for α-Fe is consistent with a MCD response that is temperature independent except for the reduced coercivity at higher temperatures. The value of $T_b=43$ K for Fe_3O_4 suggests that these particles should become superparamagnetic above 43 K. Some superparamagnetism is evident in the case of the Fe_3O_4 particles—the saturation value of the MCD decreases by 10%–20% between 4 and 298 K—but some small hysteresis indicative of ferrimagnetism persists to 297 K. This room temperature hysteresis is not unreasonable since Mössbauer measurements have confirmed that 8.2 nm particles are ferrimagnetic at room temperature, and a larger K value of 44×10^5 erg/cm^3 has been reported for the 8.2 nm particles.[7] The present samples contain some Fe_3O_4 particles at least as large as 9 nm, and their volume of 7.3×10^{-19} cm^3 when used with the larger K value in Eq. (4) gives a higher value of $T_b\cong232$ K. Because of their much larger volumes, the larger-diameter particles contribute proportionately more to the MCD, and these particles remain ferrimagnetic to much higher temperatures than do the smaller particles.

The differences between the MCD-determined hysteresis curves shown in Fig. 3 for α-Fe and Fe_3O_4 are due primarily to the intrinsic differences in the magnetic properties as well as the significant difference in the precipitate size for the two materials. There are previous reports of the formation of precipitates of α-Fe in an Al_2O_3 host by ion implantation and annealing[8] but this system was only characterized using Mössbauer spectroscopy or vibrating-sample magnetometer methods. The magneto-optical effect reported here for Fe and Fe_3O_4 particles is apparently a general phenomenon that is characteristic of magnetic nanocomposite surfaces, and the α-Fe particles produced in single crystals of Al_2O_3[8] are expected to exhibit similar optical effects.

Research sponsored by the Oak Ridge National Laboratory, managed by UT-Battelle, LLC, for the U.S. Department of Energy under Contract No. DE-AC05-00OR22725.

[1] L. A. Gea, S. Honda, L. A. Boatner, T. E. Haynes, B. C. Sales, F. A. Modine, A. Meldrum, J. D. Budai, and L. Beckers, Mater. Res. Soc. Symp. Proc. **501**, 137 (1998).
[2] L. A. Gea, L. A. Boatner, H. M. Evans, and R. Zuhr, Nucl. Instrum. Methods Phys. Res. B **127/128**, 553 (1997).
[3] L. A. Gea and L. A. Boatner, Appl. Phys. Lett. **68**, 3081 (1996).
[4] J. F. Zeigler, *Transport and Range of Ions in Matter, Version 96.01*, IBM-Research, Yorktown, NY, 1996.
[5] S. Honda, L. A. Boatner, T. E. Haynes, A. Meldrum, and F. A. Modine, (unpublished).
[6] F. Bodker, S. Morup, and S. Linderoth, Phys. Rev. Lett. **72**, 282 (1994).
[7] H. S. Lee, W. S. Lee, and T. Furubayashi, J. Appl. Phys. **85**, 5231 (1999).
[8] M. Ohkubo, T. Hioki, N. Suzuki, T. Ishiguro, and J. Kawamoto, Nucl. Instrum. Methods Phys. Res. B **39**, 675 (1989).

Downloaded 11 Sep 2009 to 160.91.157.167. Redistribution subject to AIP license or copyright; see http://apl.aip.org/apl/copyright.jsp